

Dynamical Casimir effect for magnons in a spinor Bose-Einstein condensate

Hiroki Saito¹ and Hiroyuki Hyuga²¹Department of Applied Physics and Chemistry, The University of Electro-Communications, Tokyo 182-8585, Japan²Department of Physics, Keio University, Yokohama 223-8522, Japan

(Dated: February 20, 2024)

Magnon excitation in a spinor Bose-Einstein condensate by a driven magnetic field is shown to have a close analogy with the dynamical Casimir effect. A time-dependent external magnetic field amplifies quantum fluctuations in the magnetic ground state of the condensate, leading to magnetization of the system. The magnetization occurs in a direction perpendicular to the magnetic field breaking the rotation symmetry. This phenomenon is numerically demonstrated and the excited quantum field is shown to be squeezed.

PACS numbers: 03.75.Mn, 03.70.+k, 42.50.Lc, 42.50.Dv

I. INTRODUCTION

Vacuum fluctuations play an important role in a variety of situations in quantum physics. For instance, the static Casimir effect [1] originates from vacuum fluctuations in the electromagnetic field and in the electronic states in matter. If the definition of the vacuum state depends on time due to a time-dependent external condition and the system cannot follow the instantaneous vacuum state adiabatically, the vacuum fluctuation materializes as real particles [2, 3, 4, 5]. This phenomenon is called the nonstationary or dynamical Casimir effect (DCE).

The DCE has been extensively studied [6], especially for photons and the massless scalar field. When the mirror of an optical cavity is rapidly moved [7] or the dielectric constant of the matter in a cavity is rapidly altered [8, 9, 10, 11], photons are created in the cavity even if the initial state of the electromagnetic field is in the vacuum state. The generated photons are in a squeezed state [12], which modifies the Casimir force exerted on the mirrors [13]. The finite temperature correction to the DCE [14] and decoherence via the DCE [15] have also been studied. Since there is no intrinsic Hamiltonian in the original formulation of the moving mirror problem [4], the effective Hamiltonian approach has been developed [16, 17, 18, 19]. We have derived an effective Hamiltonian for the moving mirror problem by quantizing both the electromagnetic field and the polarization field in the mirrors [20].

However, photon creation by the DCE has not yet been experimentally observed. This is because the mirror of a cavity must be vibrated at a frequency of the order of GHz (at least for a microwave cavity) in order to resonantly amplify the photon field [21]. Recently, the INFN group [22] proposed a method to detect the DCE using a semiconductor layer illuminated by laser pulses, which enables the rapid displacement of the position of the cavity mirror. The proposed experiment using this method, however, has not been completed to date.

In the present paper, we propose a novel system to realize the DCE: a Bose-Einstein condensate (BEC) of an ultracold atomic gas with spin degrees of freedom.

In this system, magnons are created through the DCE. The time-dependent external condition that causes the DCE corresponds to the time-dependent magnetic field applied to the BEC. Unlike in the case of photons, the typical energy of magnons in a BEC for a magnetic field of 1 G is $\hbar 100 \text{ Hz}$ (\hbar : Planck constant). Magnetic field modulation at this frequency is experimentally feasible. Continuous amplification of magnons by an oscillating magnetic field leads to magnetization of the system, which can be observed by *in situ* measurements [23].

In a broad sense, quasiparticle excitations in a nonstationary BEC may be regarded as the DCE. For example, a time-dependent trapping potential [24], a rapid increase in the interatomic interaction [25], and collapse of a BEC by an attractive interaction [26] generate Bogoliubov quasiparticles. In these cases, the BEC itself is also excited and its shape depends on time, whose dynamics is described by the mean-field Gross-Pitaevskii (GP) equation. However, it is difficult to distinguish the quasiparticle excitation from the mean-field excitation, and therefore these systems are unsuitable for demonstrating the DCE. In contrast, in our model, the time-dependent magnetic field excites only the vacuum fluctuation in the initial quasiparticle vacuum state, giving an ideal testing ground for the DCE.

This paper is organized as follows. Section II formulates the problem. Section III discusses the relation of the magnon excitation in the present system with the DCE. Section IV numerically demonstrates the proposed phenomena using the GP equation with quantum fluctuations. Section V provides discussion and conclusions.

II. FORMULATION OF THE PROBLEM

A. Hamiltonian for the system

We consider spin-1 bosonic atoms with mass M confined in an optical trapping potential $U(\mathbf{r})$. The single-particle part of the Hamiltonian without a magnetic field

is given by

$$\hat{H}_0 = \sum_{m=-1}^1 \int d\mathbf{r} \hat{\psi}_m^\dagger(\mathbf{r}) \left[\frac{\hbar^2}{2M} \nabla^2 + U(\mathbf{r}) \right] \hat{\psi}_m(\mathbf{r}); \quad (1)$$

where $\hat{\psi}_m(\mathbf{r})$ is the field operator that annihilates an atom with spin magnetic quantum number $m = -1; 0; 1$ at the position \mathbf{r} .

The interatomic interaction for ultracold spin-1 atoms is described by the s-wave scattering lengths a_0 and a_2 , where the subscripts 0 and 2 indicate the total spin of two colliding atoms. The interaction Hamiltonian can be written in spin-independent and spin-dependent parts as [27, 28]

$$\hat{H}_{\text{int}} = \int d\mathbf{r} c_0 \hat{\psi}^2(\mathbf{r}) + c_1 \hat{\mathbf{F}}(\mathbf{r}) \cdot \hat{\mathbf{F}}(\mathbf{r}); \quad (2)$$

where the symbol $::$ denotes the normal ordering and

$$\hat{\mathbf{F}}(\mathbf{r}) = \sum_{m=-1}^1 \hat{\psi}_m^\dagger(\mathbf{r}) \hat{\mathbf{F}}_m(\mathbf{r}); \quad (3)$$

$$\hat{\mathbf{F}}(\mathbf{r}) = \sum_{m,m'} \hat{\psi}_m^\dagger(\mathbf{r}) \hat{\mathbf{f}}_{mm'} \hat{\psi}_{m'}(\mathbf{r}); \quad (4)$$

with $\mathbf{f} = (f_x; f_y; f_z)$ being the vector of the spin-1 matrices. The interaction coefficients c_0 and c_1 in Eq. (2) are given by

$$c_0 = \frac{4}{M} \frac{\hbar^2 a_0 + 2a_2}{3}; \quad (5)$$

$$c_1 = \frac{4}{M} \frac{\hbar^2 a_2}{3} a_0; \quad (6)$$

We restrict ourselves to the case of the hyperfine spin $F = 1$ of an alkali atom with nuclear spin $I = 3/2$ and electron spin $S = 1/2$ (e.g., ^{23}Na and ^{87}Rb). Because of the hyperfine coupling between the nuclear and electron spins and their different magnetic moments, the Zeeman energy is a nonlinear function of B [29]. Taking the first and second order terms, the Hamiltonian becomes

$$\hat{H}_B = \int d\mathbf{r} p_1 B(t) \hat{F}_z + p_2 B^2(t) \hat{\psi}_1^\dagger \hat{\psi}_1 + \hat{\psi}_{-1}^\dagger \hat{\psi}_{-1}; \quad (7)$$

where p_1 and p_2 are the linear and quadratic Zeeman coefficients, respectively, and we assume that the uniform magnetic field $B(t)$ is applied in the z direction. We define the quadratic Zeeman energy as

$$q(t) = p_2 B^2(t); \quad (8)$$

which is positive for the $F = 1$ hyperfine state.

Thus, the total Hamiltonian has the form

$$\hat{H} = \hat{H}_0 + \hat{H}_B + \hat{H}_{\text{int}}; \quad (9)$$

Since the linear Zeeman term in Eq. (7) commutes with the other part of the Hamiltonian and only rotates the spin uniformly around the z axis, we neglect the linear Zeeman term henceforth.

B. Bogoliubov approximation

The initial state considered in the present paper is the ground state for an initial value of the quadratic Zeeman energy, $q = q(0)$, under the restriction

$$\int d\mathbf{r} \hat{F}_z(\mathbf{r}) = 0; \quad (10)$$

In Sec. V we discuss how to generate this state. The spin-independent interaction coefficient c_0 must be positive for the existence of the ground state. Either for $c_1 > 0$ or for $c_1 < 0$ and $q > 2j_1 j_z$, where j is a typical atomic density, almost all atoms are in the $m = 0$ state for this initial state [30]. We therefore employ the Bogoliubov approximation by setting

$$\hat{\psi}_0(\mathbf{r}) = e^{i\mathbf{t} \cdot \mathbf{h}} \phi_0(\mathbf{r}) + \hat{\psi}_0^{(1)}(\mathbf{r}); \quad (11)$$

$$\hat{\psi}_{\pm 1}(\mathbf{r}) = e^{i\mathbf{t} \cdot \mathbf{h}} \hat{\psi}_{\pm 1}(\mathbf{r}); \quad (12)$$

where $\phi_0(\mathbf{r})$ is a real function that minimizes the energy functional,

$$E_0 = \int d\mathbf{r} \phi_0 \left[\frac{\hbar^2}{2M} \nabla^2 + U(\mathbf{r}) \right] \phi_0 + \frac{c_0}{2} \phi_0^4; \quad (13)$$

is the chemical potential,

$$\mu = \int d\mathbf{r} \phi_0 \left[\frac{\hbar^2}{2M} \nabla^2 + U(\mathbf{r}) \right] \phi_0 + c_0 \phi_0^4; \quad (14)$$

and $\hat{\psi}_m(\mathbf{r})$ are the fluctuation operators. The wave function $\phi_0(\mathbf{r})$ is normalized as $\int d\mathbf{r} \phi_0^2(\mathbf{r}) = N$ with N being the number of atoms. The Heisenberg equations of motion for $\hat{\psi}_m$ are then written as [27]

$$i\hbar \frac{\partial \hat{\psi}_0}{\partial t} = \left[\frac{\hbar^2}{2M} \nabla^2 + U(\mathbf{r}) \right] \hat{\psi}_0 + c_0 \phi_0^2 \hat{\psi}_0 + \hat{\psi}_0^\dagger \hat{\psi}_0^\dagger; \quad (15)$$

$$i\hbar \frac{\partial \hat{\psi}_{\pm 1}}{\partial t} = \left[\frac{\hbar^2}{2M} \nabla^2 + U(\mathbf{r}) + q + c_0 \phi_0^2 \right] \hat{\psi}_{\pm 1} + c_1 \phi_0^2 \hat{\psi}_{\pm 1} + \hat{\psi}_{\mp 1}^\dagger; \quad (16)$$

where we neglect the second and third orders of $\hat{\psi}_m$. Equation (15) is identical with that of a scalar BEC, which gives the Bogoliubov spectrum $E_k^{(0)} = \sqrt{\epsilon_k(\epsilon_k + 2c_0 \phi_0^2)}$ for a uniform system, where $\epsilon_k = \hbar^2 k^2 / (2M)$.

If q is constant in time, we can solve Eq. (16) by setting

$$\hat{\psi}_{\pm 1} = \sum_{\mathbf{k}} \hat{b}_{\mathbf{k}} e^{i\mathbf{k} \cdot \mathbf{r}}; e^{-iE_k^{(1)} t} \hat{b}_{\mathbf{k}}^\dagger; e^{iE_k^{(1)} t} \hat{b}_{\mathbf{k}}; \quad (17)$$

where $\hat{b}_{\mathbf{k}}$ are bosonic operators for quasiparticles and u, v , and $E_k^{(1)}$ are determined by the Bogoliubov-de

Genne equations,

$$\frac{\hbar^2}{2M} r^2 + U + q + c_0 \frac{\partial^2}{\partial z^2} + c_1 \frac{\partial^2}{\partial z^2} u + c_1 \frac{\partial^2}{\partial z^2} v = E^{(1)} u; \quad (18)$$

$$\frac{\hbar^2}{2M} r^2 + U + q + c_0 \frac{\partial^2}{\partial z^2} + c_1 \frac{\partial^2}{\partial z^2} v + c_1 \frac{\partial^2}{\partial z^2} u = E^{(1)} v; \quad (19)$$

The quasiparticles created by \hat{b}_+^y , are excitations of $m = 1$ states, which we call magnons.

For a uniform system, Eqs. (18) and (19) are solved to give

$$u_k = \frac{e^{ik \cdot r}}{2V} \frac{\hbar^2 k^2 + U + q + c_1 \frac{\partial^2}{\partial z^2}}{E_k^{(1)} + 1}; \quad (20)$$

$$v_k = \frac{e^{ik \cdot r}}{2V} \frac{\hbar^2 k^2 + U + q + c_1 \frac{\partial^2}{\partial z^2}}{E_k^{(1)}}; \quad (21)$$

where V is the volume of the system and

$$E_k^{(1)} = \frac{q}{(\hbar^2 k^2 + q)(\hbar^2 k^2 + q + 2c_1 \frac{\partial^2}{\partial z^2})}; \quad (22)$$

When all Bogoliubov energies are real, the system is dynamically stable. If $c_1 < 0$ and $q < 2\hbar^2 j_1^2$, Eq. (22) is imaginary for long wavelengths and the system is dynamically unstable against spontaneous magnetization [31, 32]. In the present paper, we consider such parameters that the system is dynamically stable.

C. Effective Hamiltonian for oscillating q

Here we assume that the quadratic Zeeman energy $q(t)$ oscillates as

$$q(t) = q_0 (1 + q \sin t) \quad (23)$$

through the oscillation of the strength of the applied magnetic field. For $q = 0$, the Bogoliubov Hamiltonian for magnons is given by

$$\hat{H}_{mag}^{q=0} = \sum_k E_k^{(1)} \hat{b}_+^y \hat{b}_+ + \hat{b}_-^y \hat{b}_-; \quad (24)$$

where $E_k^{(1)}$, \hat{b}_+^y , and \hat{b}_-^y are energies and annihilation operators of magnons defined at $q = q_0$. The magnon Hamiltonian for $q \neq 0$ is then written as

$$\hat{H}_{mag}^q = \hat{H}_{mag}^{q=0} + q_0 q \sin t \int d\mathbf{r} \hat{\psi}_1^y \hat{\psi}_1 + \hat{\psi}_1^y \hat{\psi}_1; \quad (25)$$

When the last term in Eq. (25) is treated as the perturbation, its interaction representation becomes

$$\begin{aligned} & q_0 q \sin t \int d\mathbf{r} e^{i(E_k^{(1)} - E_{k'}^{(1)})t} (\hat{u} \hat{u} + \hat{v} \hat{v}) \\ & \hat{b}_+^y \hat{b}_+ + \hat{b}_-^y \hat{b}_- \\ & + e^{i(E_k^{(1)} + E_{k'}^{(1)})t} (\hat{u} \hat{v} + \hat{v} \hat{u}) \hat{b}_+ \hat{b}_- \\ & + H.c. + \text{const.}; \end{aligned} \quad (26)$$

where $H.c.$ denotes the Hermitian conjugate of the preceding term. If the frequency is resonant with $(E_k^{(1)} + E_{k'}^{(1)}) = \hbar$ for some k and k' , the terms proportional to $\hat{b}_+ \hat{b}_-$ and $\hat{b}_+^y \hat{b}_-^y$ become dominant.

When the system is uniform and is resonant with $2E_k^{(1)} = \hbar$, the Hamiltonian in Eq. (26) reduces to

$$\hat{H}_e = i q_0 V \sum_k \hat{b}_+ \hat{b}_- \hat{b}_+^y \hat{b}_-^y; \quad (27)$$

where \sum_k denotes that the summation is taken for $\hbar^2 k^2 = (2M)^{-1} \hbar$. The form of Eq. (27) suggests that the magnon state develops into the squeezed state by the oscillation of q , which will be confirmed in Sec. IV B numerically.

III. RELATION WITH THE DYNAMICAL CASIMIR EFFECT

We now discuss the relation of the present system to the usual DCE.

First let us review the DCE for an electromagnetic field. The initial state is the vacuum state for some static configurations of mirrors and dielectrics. The initial expectation values of the electric and magnetic fields therefore vanish: $\langle \hat{E} \rangle = \langle \hat{H} \rangle = 0$. These operators obey the Heisenberg equations of motion,

$$\frac{\partial}{\partial t} \hat{E}(r;t) = -\nabla \cdot \hat{H}(r;t); \quad (28)$$

$$\frac{\partial}{\partial t} \hat{H}(r;t) = -\nabla \cdot \hat{E}(r;t); \quad (29)$$

where ϵ is a dielectric constant, and the electric field operator \hat{E} must vanish at the mirrors. From Eqs. (28) and (29), $\langle \hat{E} \rangle$ and $\langle \hat{H} \rangle$ always remain zero as in classical electrodynamics, whereas the vacuum fluctuation of the electromagnetic field can be amplified, leading to the creation of photons.

For the present spinor BEC system, the initial state is assumed to be the ground state satisfying Eq. (10). Since the Hamiltonian (9) has spin-rotation symmetry around the z axis, the expectation value of the transverse magnetization for the initial state vanishes: $\langle \hat{H}_+^x \rangle = 0$,

where $\hat{F}_+ = \hat{F}_x + i\hat{F}_y$. In the Bogoliubov approximation, using Eqs. (11) and (12), the magnetization operator $\hat{F}_+ = \frac{1}{2}(\hat{\gamma}_0^\dagger + \hat{\gamma}_1^\dagger)$ reduces to

$$\hat{F}_+ \approx \frac{1}{2}(\hat{\gamma}_0^\dagger + \hat{\gamma}_1^\dagger) \quad (30)$$

From Eq. (16), the Heisenberg equations of motion for \hat{F}_+ are obtained as

$$i\hbar \frac{\partial \hat{F}_+}{\partial t} = \frac{\hbar^2}{2M} r^2 + V + q(t) + c_0 \hat{\gamma}_0^\dagger \hat{\gamma}_1 \quad (31)$$

$$i\hbar \frac{\partial \hat{\gamma}_+}{\partial t} = \frac{\hbar^2}{2M} r^2 + V + q(t) + (c_0 + 2c_1) \hat{\gamma}_0^\dagger \hat{\gamma}_1 \quad (32)$$

where we define

$$\hat{\gamma}_+ = \frac{1}{\sqrt{2}}(\hat{\gamma}_0^\dagger + \hat{\gamma}_1^\dagger) \quad (33)$$

The expectation value of this operator also vanishes, $\langle \hat{\gamma}_+ \rangle = 0$, for the initial state. We find from Eqs. (31) and (32) that $\langle \hat{F}_+ \rangle$ and $\langle \hat{\gamma}_+ \rangle$ always remain zero. On the other hand, their quantum fluctuations can be amplified due to the temporal variation of $q(t)$, leading to the creation of Bogoliubov quasiparticles, i.e., magnons. Thus, the present situation is similar to that of the DCE in the electromagnetic field in that the amplification of quantum fluctuations and (quasi)particle creations occur while the expectation values of the fields remain constant ($\langle \hat{F}_+ \rangle = \langle \hat{\gamma}_+ \rangle = 0$).

What kind of excitation phenomenon can we regard as the DCE? For example, can the excitation of ripples on water in a vibrating bucket be attributed to the DCE? The answer is partially yes, because amplification of the quantum fluctuation on the water surface does occur, which creates ripples. However, this quantum excitation is overwhelmed by the classical excitation of the water surface and identification of the quasiparticle excitations should therefore be extremely difficult. Thus, the suitable condition for studying the DCE is that only the quantum fluctuation is excited and the classical field, i.e., the expectation value of the relevant quantum field, remains constant during the temporal variation of external parameters. For the electromagnetic field, $\langle \hat{H} \rangle = \langle \hat{H}^\dagger \rangle = 0$, even when the position of the mirror and $\omega(t)$ of matter are changed. The present spinor BEC system is also suitable for studying the DCE, since $\langle \hat{F}_+ \rangle = \langle \hat{\gamma}_+ \rangle = 0$ holds during the change of $q(t)$.

IV. NUMERICAL ANALYSIS

A. Mean-field theory with quantum fluctuations

In this section, we numerically demonstrate the DCE of magnons in a spinor BEC. Since performing a full

quantum many-body simulation is difficult, we employ a mean-field approximation taking into account the initial quantum fluctuations. Recently, this method was used to predict spin vortex formation through the Kibble-Zurek mechanism in magnetization of a spinor BEC [33].

The mean-field GP equations for a spin-1 BEC are given by

$$i\hbar \frac{\partial \psi_1}{\partial t} = \frac{\hbar^2}{2M} r^2 + V + q(t) + c_0 \psi_0^\dagger \psi_1 + c_1 \frac{1}{2} F_0^\dagger F_1 \quad (34)$$

$$i\hbar \frac{\partial \psi_0}{\partial t} = \frac{\hbar^2}{2M} r^2 + V + c_0 \psi_0^\dagger \psi_0 + \frac{c_1}{2} (F_+^\dagger \psi_1 + F_-^\dagger \psi_{-1}) \quad (35)$$

where $\psi_m(r;t)$ are the macroscopic wave functions and $F_\pm = F_x \pm iF_y$ are defined by the forms in Eqs. (3) and (4) in which $\hat{\gamma}_m$ are replaced by ψ_m . The initial wave function for ψ_0 is the ground state solution ψ_0^0 of Eq. (13), which is a stationary solution of Eq. (35) for $\dot{q} = 0$. Although $\langle \hat{F}_+ \rangle = 0$ for the exact many-body initial state, we do not set $\psi_1 = 0$, since the right-hand side of Eq. (34) vanishes and no time evolution is obtained.

We include a small initial noise in ψ_1 to reproduce vacuum fluctuation in magnetization within the Bogoliubov approximation. To this end, we consider the magnetic correlation function for the Bogoliubov vacuum,

$$\langle \hat{F}_+^\dagger(r) \hat{F}_-(r^0) \rangle = \frac{1}{2} \int d\mathbf{r} \psi_0^\dagger(r) \psi_0(r^0) f(r) f(r^0) \quad (36)$$

where $f(r) = u(r) + v(r)$ and we have used Eqs. (17) and (30). To find the appropriate mean-field initial states of ψ_1 , we assume the form

$$\psi_1(r) = \sum_{\mathbf{r}} [u(\mathbf{r})b_+ + v(\mathbf{r})b_-] \quad (37)$$

where b_\pm are random numbers whose probability distribution is determined below. Substituting Eq. (37) into $F_+(r)F_-(r^0)$ and taking the average with respect to the probability distribution, we obtain

$$\begin{aligned} \langle \hat{F}_+^\dagger(r) \hat{F}_-(r^0) \rangle_{\text{avg}} &= \frac{1}{2} \int d\mathbf{r} \psi_0^\dagger(r) \psi_0(r^0) \\ &\quad [f(r)f(r^0)\langle b_+ b_+ \rangle + f(r)f(r^0)\langle b_- b_- \rangle] \\ &\quad + f(r)f(r^0)\langle b_+ b_- \rangle + f(r)f(r^0)\langle b_- b_+ \rangle \\ &\quad + f(r)f(r^0)\langle b_+ b_+ \rangle + f(r)f(r^0)\langle b_- b_- \rangle : (38) \end{aligned}$$

Using the fact that both $(u;v)$ and $(u;-v)$ are solutions of Eqs. (18) and (19) and assuming that the random variables b_+ and b_- obey the same distribution, we find

that Eq. (38) coincides with Eq. (36) by a probability distribution satisfying

$$\langle \hat{b}_k; \hat{b}_k \rangle_{\text{avg}} = \frac{1}{2} \delta_{k,0}; \quad \langle \hat{b}_k; \hat{b}_k \rangle_{\text{avg}} = 0: \quad (39)$$

We also assume $\langle \hat{b}_k; \hat{b}_k \rangle_{\text{avg}} = \langle \hat{b}_k; \hat{b}_k \rangle_{\text{avg}} = 0$. Thus, the initial mean-field states (37) with probability distributions obeying Eq. (39) reproduce the same magnetic correlation as for the Bogoliubov approximation. Similarly, we can show that the time evolution of $\langle \hat{F}_+(r) \hat{F}_-(r^0) \rangle_{\text{avg}}$ also agrees with that of $\langle \hat{F}_+(r) \hat{F}_-(r^0) \rangle$ at the level of the Bogoliubov approximation.

B. Numerical results

We numerically solve Eqs. (34) and (35) for the time-dependent magnetic field that gives a sinusoidal oscillation of the quadratic Zeeman energy as in Eq. (23). For simplicity, we consider a uniform two-dimensional (2D) system with a periodic boundary condition. We assume that 10^7 ^{23}Na atoms are in a $100 \text{ m} \times 100 \text{ m}$ space with atomic density $n = 2.8 \times 10^{14} \text{ cm}^{-3}$. In a recent experiment [35], a_0 / c_1 for an $F = 1$ ^{23}Na atom was precisely measured to be about 2.47 Bohr radii. The system is therefore dynamically stable according to Eq. (22). The initial state is $\rho_0 = \rho_n$ and ρ_1 are given by Eqs. (37) and (39) in which the complex random variables b_{jk} are assumed to follow the Gaussian distribution $P(b) = \frac{1}{2\pi} e^{-2|b|^2}$. The initial random variables b_{jk} are cut off for $2\pi k < 1.5 \text{ m}$. The strength of the magnetic field at $t = 0$ is 500 mG , which corresponds to $q_0 / \hbar = 69 \text{ Hz} / 1.02 \text{ qn}$.

Figure 1 (a) shows time evolution of the average squared transverse magnetization [34],

$$G_T = \frac{R}{R} \frac{d\langle \hat{F}_+(r) \hat{F}_-(r) \rangle}{dr^2(r)}; \quad (40)$$

and longitudinal magnetization,

$$G_L = \frac{R}{R} \frac{d\langle \hat{F}_z(r) \rangle}{dr^2(r)}; \quad (41)$$

for $\omega = 2\pi \frac{q_0}{q_0 + 2c_1 n} \approx 2\pi \times 237 \text{ Hz}$ and $q_0 = 0.2$. This frequency is resonant with $2E_{k=0}^{(1)} = \hbar$, and the $k = 0$ modes are expected to be excited according to the effective Hamiltonian (27). From Fig. 1 (a), we find that the time constant for the exponential growth of G_T is $\approx 22 \text{ ms}$.

Solving the Heisenberg equation for the effective Hamiltonian with $k = 0$,

$$\hat{H}_e^0 = i_0 \hat{b}_{+0} \hat{b}_{-0} + \hat{b}_{+0}^\dagger \hat{b}_{-0}^\dagger; \quad (42)$$

we obtain

$$\hat{b}_{\pm 0}(t) = \hat{b}_{\pm 0} e^{iE_0^{(1)} t / \hbar} \cosh \omega_0 t + \hat{b}_{\mp 0}^\dagger e^{iE_0^{(1)} t / \hbar} \sinh \omega_0 t; \quad (43)$$

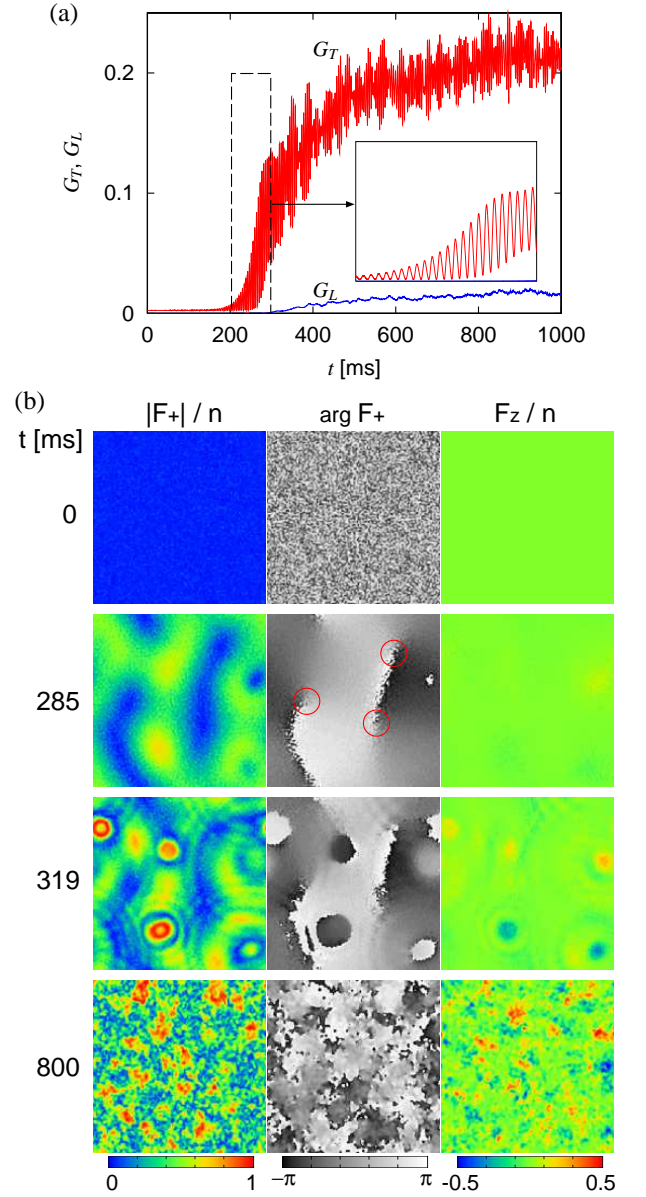


FIG. 1: (Color) (a) Time evolution of the average squared transverse magnetization G_T (red curve) and longitudinal magnetization G_L (blue curve) for $n = 2.8 \times 10^{14} \text{ cm}^{-3}$, $N = 10^7$, $\omega = 2\sqrt{q_0/(q_0 + 2c_1 n)} \times 237 \text{ Hz}$, and $q_0 = 0.2$. The inset magnifies the dashed square. (b) Profiles of $|F_+|/n$, $\arg F_+$, and F_z/n at $t = 0, 285, 319$, and 800 ms . The field of view is $100 \text{ m} \times 100 \text{ m}$. The red circles indicate the topological defects.

where $\rho_0 = q_0 / (q_0 + 2c_1 n)$. Substitution of this solution into Eq. (30) with

$$\hat{\psi}_1(r;t) = \sum_k \frac{\hbar}{u_k(r)} \hat{b}_{jk}(t) + \frac{i}{v_k(r)} \hat{b}_{jk}^\dagger(t) \quad (44)$$

gives

$$\begin{aligned} \hat{F}_+(t) &= \frac{p}{2n} \sum_{\mathbf{k}} e^{i\mathbf{k} \cdot \mathbf{r}} (\hat{b}_{\mathbf{k}} + \hat{b}_{-\mathbf{k}}) e^{i\mathbf{k} \cdot \mathbf{r}} \hat{b}_{\mathbf{k}}^\dagger(t) + \hat{b}_{-\mathbf{k}}^\dagger(t) \\ &= \frac{p}{2n} \sum_{\mathbf{k}} (\hat{b}_{\mathbf{k}} + \hat{b}_{-\mathbf{k}}) e^{i\mathbf{k} \cdot \mathbf{r}} e^{i\mathbf{k} \cdot \mathbf{r}} e^{i\mathbf{k} \cdot \mathbf{r}} e^{i\mathbf{k} \cdot \mathbf{r}} \\ &= \frac{p}{2n} \sum_{\mathbf{k}} (\hat{b}_{\mathbf{k}} + \hat{b}_{-\mathbf{k}}) e^{i\mathbf{k} \cdot \mathbf{r}} e^{i\mathbf{k} \cdot \mathbf{r}} e^{i\mathbf{k} \cdot \mathbf{r}} e^{i\mathbf{k} \cdot \mathbf{r}}; \quad (45) \end{aligned}$$

where in the second line we take only the $\mathbf{k} = 0$ component because of the exponential factor $e^{i\mathbf{k} \cdot \mathbf{r}}$. The average squared transverse magnetization G_T thus grows exponentially with a time constant $\tau = (2\gamma)^{-1} = 20$ ms, which is in good agreement with the numerical results of 22 ms.

The spatial profile of the magnetization is shown in Fig. 1 (b). The transverse magnetization first grows with long wavelength [the second row of Fig. 1 (b)], in which we can see a few topological defects (red circles). These spin vortices are generated through the Kibble-Zurek mechanism [33, 36]. The transverse magnetization then exhibits an interesting concentric pattern [the third row of Fig. 1 (b)], which may be due to the nonlinearity. The magnetization finally breaks into complicated fragments and the longitudinal magnetization also begins to grow [the fourth row of Fig. 1 (b)].

We now discuss symmetry breaking in the DCE. The original Hamiltonian (9) commutes with \hat{F}_z and the system has spin-rotation symmetry around the z axis. In reality, however, local magnetization in the x - y directions occurs in a ferromagnetic BEC breaking the spin-rotation symmetry spontaneously [34], and we expect that the symmetry breaking also occurs in the present system. This is because the exact quantum state with spin-rotation symmetry is the macroscopic superposition of magnetized states in the x - y directions, which is therefore fragile against external perturbations. Such symmetry breaking phenomena should also occur in the DCE of the electromagnetic field. For example, in the 1D moving mirror problem [7], there is rotation symmetry around the axis of the 1D cavity and the generated photon state is a superposition of all polarizations, giving $\langle \hat{E}_x \rangle = \langle \hat{E}_y \rangle = 0$. When we measure the local electromagnetic field, however, we obtain a nonzero value as a result of the symmetry breaking.

Figure 2 shows the magnitude of the Fourier transform of F_+ ,

$$\tilde{F}_+(\mathbf{k}) = \frac{1}{V} \int d\mathbf{r} F_+(\mathbf{r}) e^{i\mathbf{k} \cdot \mathbf{r}}; \quad (46)$$

Initially only the $\mathbf{k} = 0$ modes grow as shown in Fig. 2 (a). Then, the momentum distribution becomes broad as shown in Fig. 2 (b). Specific wave numbers can be selectively excited using larger γ . Figure 2 (c) shows the result for $\gamma = 2\pi \times 358$ Hz, which is resonant with $2E_k^{(1)} = \hbar$ for $k = 0.5 \text{ nm}^{-1}$. We can see the ring at this wave number.

From the form of the effective Hamiltonian in Eq. (27), generated magnons are expected to have quantum corre-

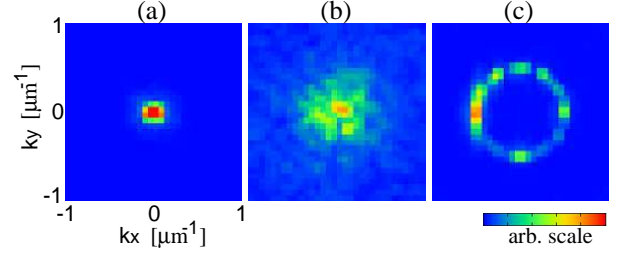


FIG. 2: (Color) Magnitude of the Fourier transform of F_+ at (a) $t = 285$ ms and (b) $t = 800$ ms. The parameters are the same as in Fig. 1. (c) Magnitude of the Fourier transform of F_+ at $t = 500$ ms for $\gamma = 2\pi \times 358$ Hz. The other parameters are the same as in Fig. 1.

lations. Defining new operators,

$$\hat{B}_{+\mathbf{k}} = \frac{1}{\sqrt{2}} (\hat{b}_{+\mathbf{k}} + \hat{b}_{-\mathbf{k}}); \quad (47)$$

$$\hat{B}_{-\mathbf{k}} = \frac{1}{\sqrt{2}} (\hat{b}_{+\mathbf{k}} - \hat{b}_{-\mathbf{k}}); \quad (48)$$

we can rewrite Eq. (27) as

$$\hat{H}_e = \sum_{\mathbf{k}} \frac{1}{2} \left(\hat{B}_{+\mathbf{k}}^2 + \hat{B}_{-\mathbf{k}}^2 + \hat{B}_{+\mathbf{k}}^{\dagger 2} + \hat{B}_{-\mathbf{k}}^{\dagger 2} \right); \quad (49)$$

where $\mathbf{k} = \mathbf{q} + \mathbf{G}$, \mathbf{G} is a reciprocal lattice vector. We can clearly see that this Hamiltonian generates the squeezed state.

Figure 3 (a) plots the values of $B_{+\mathbf{k}} = (\hat{b}_{+\mathbf{k}} + \hat{b}_{-\mathbf{k}})/\sqrt{2}$ at $t = 0$ and 30 ms. The distribution of $B_{+\mathbf{k}}$ corresponds to the quantum fluctuation in Eq. (47) with $\mathbf{k} = 0$, which is expected to be squeezed. The values of $b_{-\mathbf{k}}$ are obtained from $b_{-\mathbf{k}} = \frac{1}{\sqrt{2}} [\hat{b}_{+\mathbf{k}} - \hat{b}_{-\mathbf{k}}]$ with $\hat{b}_{-\mathbf{k}} \sim \hat{b}_{+\mathbf{k}}^\dagger$ being the Fourier transform of $\psi_-(\mathbf{r})$. Each point in Fig. 3 (a) corresponds to a single simulation run and 1000 simulations are performed. Figure 3 (b) shows the variance of $\text{Re}(B_{+\mathbf{k}} e^{i\mathbf{k} \cdot \mathbf{r}})$,

$$V(\mathbf{k}) = \langle [\text{Re}(B_{+\mathbf{k}} e^{i\mathbf{k} \cdot \mathbf{r}})]^2 \rangle_{\text{avg}} - \langle \text{Re}(B_{+\mathbf{k}} e^{i\mathbf{k} \cdot \mathbf{r}}) \rangle_{\text{avg}}^2; \quad (50)$$

For the initial state, the variance is isotropic, $V(\mathbf{k}) = 1/4$, from Eq. (39). The small deviation of the solid curve from $1/4$ in Fig. 3 (b) is the statistical error. At $t = 30$ ms, the distribution of $B_{+\mathbf{k}}$ is clearly squeezed, and the maximum and minimum values of $V(\mathbf{k})$ are 1.09 and 0.057. For the present parameters, $e^{2\gamma t} = 4.38$ at $t = 30$ ms, which is in good agreement with $1.09 = 0.25 \times 0.25 = 0.057$. Since $1.09 = 0.057 \times 1/4$, the squeezed state is almost the minimum uncertainty state.

In this section, we assumed the use of ^{23}Na atoms. Similar results can be obtained also for $F = 1$ ^{87}Rb atoms with a ferromagnetic interaction ($c_1 < 0$), where $q(t)$ must always be larger than $j_1 j_0^2$ in order to suppress the spontaneous magnetization.

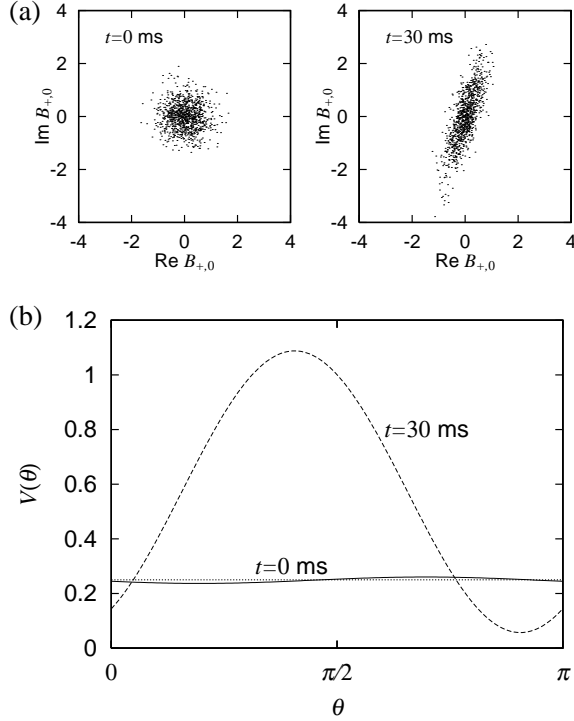


FIG. 3: (a) Distributions of $B_{+,0} = (b_{+,0} + b_{-,0})e^{i\theta}$ at $t = 0$ and 30 ms obtained by 1000 simulation runs with different initial states produced by random numbers. The parameters are the same as in Fig. 1. (b) Variance $V(\theta)$ of $\text{Re}(B_{+,0}e^{-i\theta})$ for the data in (a). The dotted line indicates $V(\theta) = 1/4$.

V. DISCUSSION AND CONCLUSIONS

We now discuss the possibility of experimental observation of the proposed phenomena. The magnetization profile $F(r)$ as shown in Fig. 1 can be measured by spin-sensitive phase-contrast imaging in a nondestructive manner [23, 34], from which G_T , G_L , and $\tilde{F}(k)$ are obtained. The squeezing of the field as shown in Fig. 3 can also be observed. From Eq. (45), we can measure both $b_{+jk} + b_{-jk}$ and $b_{+jk} - b_{-jk}$, and therefore we obtain B_{+jk} . In order to assure that the observed magnetization is definitely due to amplification of the vacuum fluctua-

tion, we must prepare the appropriate initial state. In principle, the initial magnon vacuum state can be prepared as follows. First, a BEC is prepared in the $m = 0$ state at a sufficiently strong magnetic field ($q \ll c_1^2/0$), in which the $m = 0$ state is almost the ground state. The residual atoms in the $m = \pm 1$ states must be eliminated completely. Then, the magnetic field is adiabatically decreased to the desired strength, which gives a magnon vacuum state satisfying Eq. (10).

In conclusion, we have studied the magnon excitation in a spinor BEC by a driven external magnetic field and have demonstrated the close analogy of this phenomenon with the DCE. The present system is suitable for studying the DCE of quasiparticles, since the time-dependent magnetic field applied to the Bogoliubov ground state amplifies only the vacuum fluctuation, keeping the "classical fields" constant in the Bogoliubov approximation.

We numerically demonstrated magnon excitation in a spinor BEC using the mean-field GP equation, in which the vacuum fluctuation is taken into account by the initial random noise. We have shown that the oscillating external magnetic field resonantly amplifies the vacuum fluctuation, leading to magnetization of the system (Fig. 1). The Fourier transform of the excited field reveals that the specific wave number k can be selectively amplified (Fig. 2). The excited quantum field is squeezed (Fig. 3) as in the DCE of photons. The growth of magnetization in Fig. 1 (a) and the degree of squeezing in Fig. 3 can be well described by the effective Hamiltonian in Eq. (27).

A spinor BEC is thus a good testing ground for the DCE and our proposal is feasible with current experimental techniques. Study of the DCE of quasiparticles may serve as a stepping stone to the observation of the DCE of photons.

Acknowledgments

This work was supported by the Ministry of Education, Culture, Sports, Science and Technology of Japan (Grants-in-Aid for Scientific Research, No. 17071005 and No. 20540388) and by the Matsuo Foundation.

[1] H. B. G. Casimir, *Proc. K. Ned. Akad. Wet.* 51, 793 (1948).
[2] Y. Takahashi and H. Umezawa, *Nuovo Cimento* 6, 1324 (1957).
[3] L. Parker, *Phys. Rev. Lett.* 21, 562 (1968).
[4] G. T. Moore, *J. Math. Phys.* 11, 2679 (1970).
[5] S. A. Fulling and P. C. W. Davies, *Proc. R. Soc. London A* 348, 393 (1976).
[6] For review, see, V. V. Dodonov, *Adv. Chem. Phys.* 119, 309 (2001); V. V. Dodonov and A. V. Dodonov, *J. Phys.: Conf. Ser.* 99, 012006 (2008).
[7] See, e.g., M. Castagnino and R. Ferraro, *Ann. Phys.*

(N.Y.) 154, 1 (1984); V. V. Dodonov, A. B. Klimov, and D. E. Nikonov, *J. Math. Phys.* 34, 2742 (1993); C. K. Law, *Phys. Rev. Lett.* 73, 1931 (1994).
[8] E. Yablunovitch, *Phys. Rev. Lett.* 62, 1742 (1989).
[9] V. V. Dodonov, A. B. Klimov, and D. E. Nikonov, *Phys. Rev. A* 47, 4422 (1993).
[10] H. Johnston and S. Sarkar, *Phys. Rev. A* 51, 4109 (1995).
[11] H. Saito and H. Hyuga, *J. Phys. Soc. Jpn.* 65, 1139 (1996); *ibid.* 65 3513 (1996).
[12] V. V. Dodonov, A. B. Klimov, and V. I. Man'ko, *Phys. Lett. A* 149, 225 (1990).
[13] M. T. Jaekel and S. Reynaud, *J. Phys. I France* 2, 149

- (1992).
- [14] G. P. Lünien, R. Schützhold, and G. So, Phys. Rev. Lett. 84, 1882 (2000).
 - [15] D. A. R. Dalvit and P. A. Maia Neto, Phys. Rev. Lett. 84, 798 (2000).
 - [16] M. Razavy, Lett. Nuovo Cimento 37, 449 (1983).
 - [17] G. Barton and C. Eberlein, Ann. Phys. (N.Y.) 227, 222 (1993).
 - [18] C. K. Law, Phys. Rev. A 49, 433 (1994).
 - [19] J. Haro and E. Elizalde, Phys. Rev. Lett. 97, 130401 (2006).
 - [20] H. Saito and H. Hyuga, Phys. Rev. A 65, 053804 (2002).
 - [21] V. V. Dodonov and A. B. Klimov, Phys. Rev. A 53, 2664 (1996).
 - [22] C. Braggio, G. Bressi, G. Carugno, C. Del Noce, G. Galeazzi, A. Lombardi, A. Palmieri, G. Ruoso, and D. Zanello, Europhys. Lett. 70, 754 (2005).
 - [23] J. M. Higbie, L. E. Sadler, S. Inouye, A. P. Chikkatur, S. R. Leslie, K. L. Moore, V. Savalli, and D. M. Stamper-Kum, Phys. Rev. Lett. 95, 050401 (2005).
 - [24] Y. Castin and R. Dum, Phys. Rev. Lett. 79, 3553 (1997).
 - [25] C. K. Law, P. T. Leung, and M. -C. Chu, Phys. Rev. A 66, 033605 (2002).
 - [26] E. A. Calzetta and B. L. Hu, Phys. Rev. A 68, 043625 (2003).
 - [27] T. -L. Ho, Phys. Rev. Lett. 81, 742 (1998).
 - [28] T. Ohmachi and K. Machida, J. Phys. Soc. Jpn. 67, 1822 (1998).
 - [29] See, e.g., C. J. Pethick and H. Smith, Bose-Einstein Condensation in Dilute Gases (Cambridge Univ. Press, Cambridge, 2002).
 - [30] J. Stenger, S. Inouye, D. M. Stamper-Kum, H. -J. Miesner, A. P. Chikkatur, and W. Ketterle, Nature (London) 396, 345 (1998).
 - [31] H. Saito and M. Ueda, Phys. Rev. A 72, 023610 (2005).
 - [32] H. Saito, Y. Kawaguchi, and M. Ueda, Phys. Rev. Lett. 96, 065302 (2006); Phys. Rev. A 75, 013621 (2007).
 - [33] H. Saito, Y. Kawaguchi, and M. Ueda, Phys. Rev. A 76, 043613 (2007).
 - [34] L. E. Sadler, J. M. Higbie, S. R. Leslie, M. Vengalattore, and D. M. Stamper-Kum, Nature (London) 443, 312 (2006).
 - [35] A. T. Black, E. Gomez, L. D. Toner, S. Jung, and P. D. Lett, Phys. Rev. Lett. 99, 070403 (2007).
 - [36] B. Damski and W. H. Zurek, Phys. Rev. Lett. 99, 130402 (2007).